Proceedings of Global Power and Propulsion Society
ISSN-Nr: 2504-4400
GPPS Hong Kong 2023
October 17-19, 2023
www.gpps.global

GPPS-TC-2023-0084

ANALYSIS OF HIGH TEMPERATURE FLANGE & BOLT TEMPERATURE VARIATION OF THE STEAM TURBINE CYLINDER DURING START-UP PROCESS BASED ON IN-SERVICE DATA

Ming Kang[1,2]
Shanghai Jiao Tong University,School of Mechanical and Power Engineering[1]
kangming@sjtu.edu.cn
Shanghai, China

Shi-Fang Wu[1,2]
Shanghai Electric Power Generation Equipment Co., Ltd. Shanghai Turbine Plant[2]
wushf@shanghai-electric.com
Shanghai, China

Geng-Hui Jiang[1]
Shanghai Jiao Tong University, School of Mechanical and Power Engineering[1]
ghjiang@sjtu.edu.cn
Shanghai, China

Wei-Zhe Wang[1]
Shanghai Jiao Tong University, School of Mechanical and Power Engineering[1]
wangwz0214@sjtu.edu.cn
Shanghai, China

ABSTRACT

In order to monitor the temperature and temperature difference levels of the flange-bolt components in the cylinder's joint surface during start-up process, temperature measurement elements are installed at different depths of the flange and at different heights of the bolt. The temperature of each measurement point and the temperature difference between the measurement points are analyzed in the cold start, warm start and hot start modes with the unit in-service data. The maximum temperature difference between the flange-bolt, between different depths of the flange and between different heights of the bolt in the warm start mode is higher than the maximum temperature difference values corresponding to the cold start and the hot start mode, which corresponds to a maximum temperature difference of 110 °C between the flange and the bolt, 70 °C between different depths of the flange and 28 °C between different heights of the bolt. The results of the study are important for understanding the temperature change pattern of the flange-bolt structure system of the cylinder during the start-up phase, and also provide guidance for its structural strength assessment and high temperature creep fatigue life assessment.

INTRODUCTION

In response to global climate change, in 2020 China proposed the goal of peaking carbon emissions by 2030 and achieving carbon neutrality by 2060, i.e. the "3060 Double Carbon" target. To this end, the total installed capacity of new energy sources such as wind and solar power in China is expected to reach over 1.2 billion kW in 2030 (Zhao B et al.,2022). In order to cope with the impact of the random, intermittent and unstable nature of new energy generating units on the grid, and to ensure the stability of the entire grid system, coal-fired generating units and gas-steam combined cycle units, which carry the base load, are frequently involved in the load and frequency regulation of the grid. In order to accurately assess the impact of complex alternating loads generated by frequent load fluctuation operation of the unit on the safety and reliability of the high temperature flange-bolt structure, it is necessary to accurately assess the temperature field distribution and change patterns within the flange-bolt structural components and to study the stresses, strains and stress amplitudes within the structural components based on the temperature field distribution.

To this end, researchers have carried out a large number of theoretical and experimental studies on the temperature field of high temperature flange-bolt connection structures, etc.: Yu Jianliang et al (Yu J et al., 2013) constructed an experimental research system for high temperature flange-bolt-gasket structures and carried out experimental studies and finite element simulations on the temperature distribution of the components and the variation law of the bolt load at different flange inner wall temperatures, pointing out that a significant temperature gradient is formed along the inner wall of the flange to the outer wall of the flange at high temperatures. Yu Jiuyang et al (Yu J et al., 2014) used the finite element software ANSYS to establish a three-dimensional temperature field model of the bolt, flange and gasket connection system, and conducted a theoretical study on the temperature field distribution law of the flange-bolt structure system of the refinery

unit under the high temperature environment of 500 ℃. Hao Zhenzhen et al (Hao Z et al., 2016) studied the local conjugate heat transfer model in the local high-temperature bolt area in the middle part of the cylinder based on the steady-state calculation results by constructing a numerical model of conjugate heat transfer in the high-temperature and high-pressure module where the high-temperature and high-pressure integral inner cylinder of the turbine with H-class is located, and pointed out that the accuracy of the high-temperature bolt temperature field obtained by the numerical model of conjugate heat transfer is higher than that calculated by the traditional finite element method. Jiang Feng et al (Jiang F et al., 2021) combined heat transfer theory and ANSYS finite element analysis software, based on transient temperature field and thermal-structural coupling, established a three-dimensional finite element model and temperature field model for flanges, bolts and gaskets in the valve structure, studied the effect of different heating rates on gasket sealing, and pointed out that temperature fluctuations would lead to increased deformation and reduced stress on the inside and outside of the gasket, affecting sealing reliability. Wu Shifang et al (Wu S et al., 2021), in order to verify the accuracy of the empirical formula for the heat transfer coefficient in calculating the temperature field, combined the measured data of the temperature field and the finite element calculation results to investigate the temperature field in the inlet cavity of a medium pressure inner cylinder and the flange area of the middle division surface of an in-service turbine, and pointed out the limitations and shortcomings of the empirical heat transfer coefficient. Zhao Nailong et al (Zhao N et al., 2016) established a 3D 1:1 scaled real bolted inner casing model of a ultra-supercritical steam turbine using the commercial soft ware ABAQUS. The thermal-mechanical loading were applied based on the in-service conditions to study the influence of steam temperature and pressure fluctuations. Benjamin Leibing et al (Benjamin L et al., 2019) developed a test rig comprising a scaled intermediate pressure (IP) steam turbine pipe flange, a loss in bolt pretension of up to almost 50% over a comparatively short period of experiment time was observed. In addition, by means of numerical calculations, creep deformation in the transition areas between pipe and flange plate sections was identified to be a major originator of these pretension drops. In addition, Wolfgang F. Mohr et al (Wolfgang F. Mohr et al. 2012), propose a new method for high-temperature rotor temperature measurement, which maybe the first-in-time application of intensity pyrometry to measure in-situ the hot rotor surface temperature of a standard, combined cycle, intermediate pressure steam turbine. The pyrometric temperatures are compared to standard temperature measurements on static turbine parts and an upstream steam temperature measured on a thermo well. It is reported, how the applicability of pyrometry in steam turbines was assessed. Details are given about a newly developed USC autoclave, which was used to measure steam transmittance, and about the measurement of the emissivity of the rotor metal. Gabriel Marinescu et al (Gabriel Marinescu et al. 2012,2013,2014)， in order to assess the thermal regime and the behavior of steam turbine components during natural cooling including the steam turbine rotors, casings,valves and main pipes, a number of thermocouples and optical probes were installed on a commercial steam turbine to measure the temperatures on rotor and casings during start-up, cooling down.

The research on the temperature field of high temperature flange-bolt is mainly focused on finite element simulation and experimental research, but there is less research on the temperature change of the flange-bolt structure components in the thick-walled parts of the turbine cylinder in service, such as during the start-up process. This paper combines the service data of the metal temperature measurement points on the flange and bolt side of a turbine to study the temperature changes of the flange-bolt metal under different starting modes of cold, warm and hot states, so as to provide data support for the subsequent design of the turbine structure and the selection of high-temperature bolts.

BOUNDARY CONDITIONS

Figure 1 shows the three-dimensional structure model of the inner cylinder of an in-service turbine and the arrangement of measurement points. In order to study the temperature changes of the flange-bolt structure of the inner cylinder at each stage of operation, metal temperature measurement points are set at different depths of the flange and at different heights of the bolt in the inlet and near the discharge area of the inner cylinder. Positions 1, 2 and 3 represent the metal measurement points in the area of the inlet flange at 50% depth, 99% depth and the area of the bolt at 75% height with temperatures T1, T2 and T3 respectively; positions 4, 5 and 6 represent the metal measurement points near the area of the discharge flange at 50% depth, 99% depth and the area of the bolt at 25% height with temperatures T4, T5 and T6 respectively. Measurement points 1, 2, 4 and 5 represent metal temperature measurement points in different areas and at different depths of the flange in the upper half of the cylinder. Measurement points 2 and 5 represent the metal temperature measurement points at 99% of the flange metal thickness, where the total thickness of the flange is about 204 mm and the measurement points are arranged at a thickness of about 200 mm. Measurement points 1 and 4 represent metal temperature measurement points at 50% of the metal thickness of the flange, where the measurement points are arranged at a thickness of approximately 102 mm. Measurement points 3 and 6 represent metal temperature measurement points at different heights of the bolt. In particular, the location of the measuring point 3 is arranged essentially at the center parting of the upper and lower half flanges of the cylinder, and the location of the measuring point 6 is close to the area of the mating surface between the nut and the upper half flange of the cylinder. Here the total length of the bolt under test is 460 mm, the measuring point 3 is arranged at a height of about 122 mm and the measuring point 6 is arranged at a height of 317 mm.

The inlet pressure of the cylinder under rated operating conditions is 3.3MPa(a) and the inlet temperature is 620°C. The discharge pressure is 2.1MPa(a) and the discharge temperature is 550°C. The rated speed of the unit is 3000 r/min.

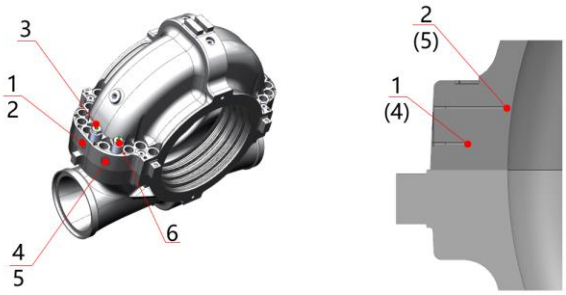

(a) Diagram of the layout of each temperature measurement point

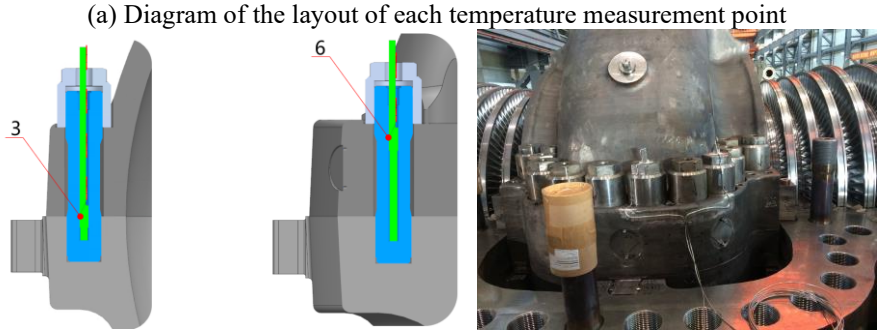

(b) Diagram of bolt temperature installation

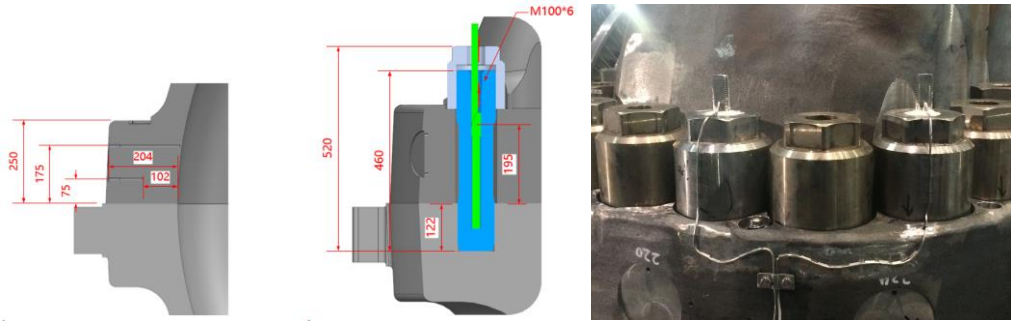

(c) Measuring point positioning and bolt construction dimensions

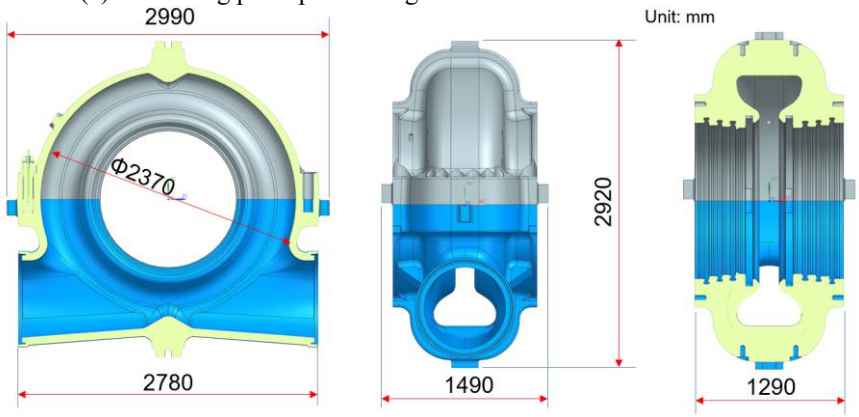

(d) Schematic diagram of the main structural dimensions of the turbine cylinder

Figure 1 Schematic diagram of the flange-bolt metal temperature measurement point arrangement on the steam turbine

The temperature field data, which changes in real time with the service of the unit, is collected by the temperature measuring element and then stored and post-processed by the data acquisition system. The temperature measuring element is a K-type armoured thermocouple with a diameter of 4mm, which has a high zero sensitivity, with a potential change of 0.04mv for every 1°C change in temperature, a nearly linear temperature characteristic, good reproducibility, high resistance to oxidation and low influence by radiation. Its temperature measurement accuracy can meet the needs of engineering applications.

RESULTS AND DISCUSSION

In order to control the stress level of high temperature and high pressure thick-walled components (e.g. cylinders) and high-speed rotating components (e.g. rotors), as well as the stress magnitude and life loss of key components during

start/stop and variable load operation, the start-up of the turbine is controlled sequentially according to the temperature margin of the corresponding equipment and X guidelines, especially for units with high Fracture Appearance Transition Temperature (FATT) of the rotor material, the start-up phase should meet the requirements of the rotor preheating control guidelines. Here, data on the flange-bolt temperature of the unit in service is selected for analysis under three typical start-up methods.

Cold start-up

Figure 2 shows the temperature trend of each measurement point over time under cold start. Before cold start, the metal temperature of the cylinder is basically maintained at around 50 °C. Here, the unit is analysed from a cumulative total of approximately 700 min of operation from turning gear operation, low-speed warm-up and idling at rated speed. In this case, measurement point 7 is the metal measurement point at 99% depth of the main valve body. As can be seen from Figure 2, when the rotor operating state is changed, such as from turning gear operation to low speed warm-up or low speed warm-up to rated speed, the temperature of the corresponding measurement points also changes sharply at the same time. In addition, with the accumulation of start-up time, the temperature of each measurement point T1 to T6 of the inner cylinder flange-bolt gradually approaches the temperature of the metal measurement point T7 at 99% of the depth of the main valve casing, and the overall temperature difference or temperature gradient between the metal temperature of the main valve casing and the metal temperature of the inner cylinder side gradually decreases. During the cold start-up period, the metal temperature at each measurement point maintains a linear increase.

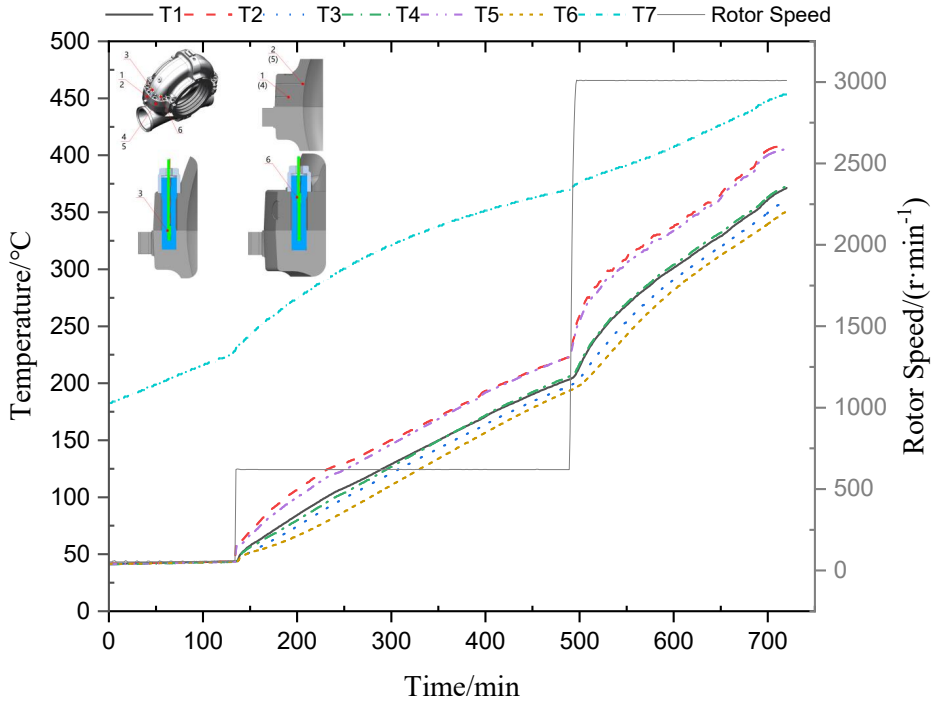

Figure 2 Diagram of temperature variation with time for cold start mode

At the beginning of the cold start, the unit is driven by the hydraulic motor and maintained in turning gear operation at 50 r/min. At this stage, as the main steam gate is closed, the temperature of the measurement points at the flange and bolts in the inner cylinder are arranged to maintain a low level, with the same measurement point data of approximately 50 °C. As the steam parameters increase, the temperature of the metal measurement point T7 at 99% depth of the main steam stop valve body also increases steadily. When the cold start time accumulates to 135 min, the steam quality (cleanliness, superheat, etc.) and the temperature margin of the main stop valve meet the unit's start-up requirements, at which point the main stop valve is fully open and the control vale is in a small open state, corresponding to a valve stroke of 4%, with a small amount of steam entering the inner cylinder and maintaining the rotor at 620 r/min for low-speed warm-up. When the cold start time accumulates to 489 min, the rotor impulse limit signal is released, the whole rotor is preheated to above FATT, the rotor material changes from a brittle state to a ductile state, the low-speed warm-up process is completed, the control valve opening is further increased, at this time the control valve's opening increases from 4% to about 16% in the low-speed warm-up phase, and the rotor ramps up from 620 r/min to 3000 r/min rated speed after 8 min.

Combined with Figure 2, it can be further concluded that during the cold start-up phase, T7 is the highest and T6 is the lowest; during the whole start-up process, the temperature of each measurement point satisfies $T2 \geqslant T5 > T1 \geqslant T4 > T3 > T6$; the distribution of the measured temperatures T1 and T4 in the 50% depth region of the flange and T2 and T5 in the 99% depth region are basically the same, and the change trend is also the same. This indicates that the temperature

field distribution in the centre split flange area has a relatively small temperature gradient along the axial direction of the cylinder. In addition, the temperature of the measurement points at the same depth and at different locations on the flange is slightly higher in the inlet area due to the high temperature steam from the lower half of the cylinder inlet.

Figure 3 illustrates the temperature variation between each measurement point of the flange-bolt in the inner cylinder. As can be seen from Figure 3, the temperature difference between the measurement points changes sharply when the rotor is ramped up from the turning gear operation state to low-speed warm-up, and when the low-speed warm-up speed ramps up to the rated speed, the main steam stop valve and control valve are all open, and high temperature and high pressure steam enters the cylinder; the temperature difference shows a non-linear trend, with the temperature difference between the measurement points increasing first and then decreasing at a certain moment when the valve opens. After entering the quasi-steady-state operating range of low-speed warm-up, the temperature difference between the measurement points changes relatively gently; after entering the idling operating range of 3000 r/min rated speed, the temperature difference between the measurement points changes relatively drastically, showing the characteristics of fluctuation changes. The temperature difference between measurement points 1 and 2 is expressed as ΔT21, and so on, comparing the temperature difference between the coiling, low-speed warm-up and rated speed idling stages, it can be seen that the temperature difference in the rated speed idling stage is the largest value. Each temperature difference satisfies $\Delta T56 \geqslant \Delta T23 > \Delta T21 > \Delta T54 > \Delta T46 > \Delta T13$.

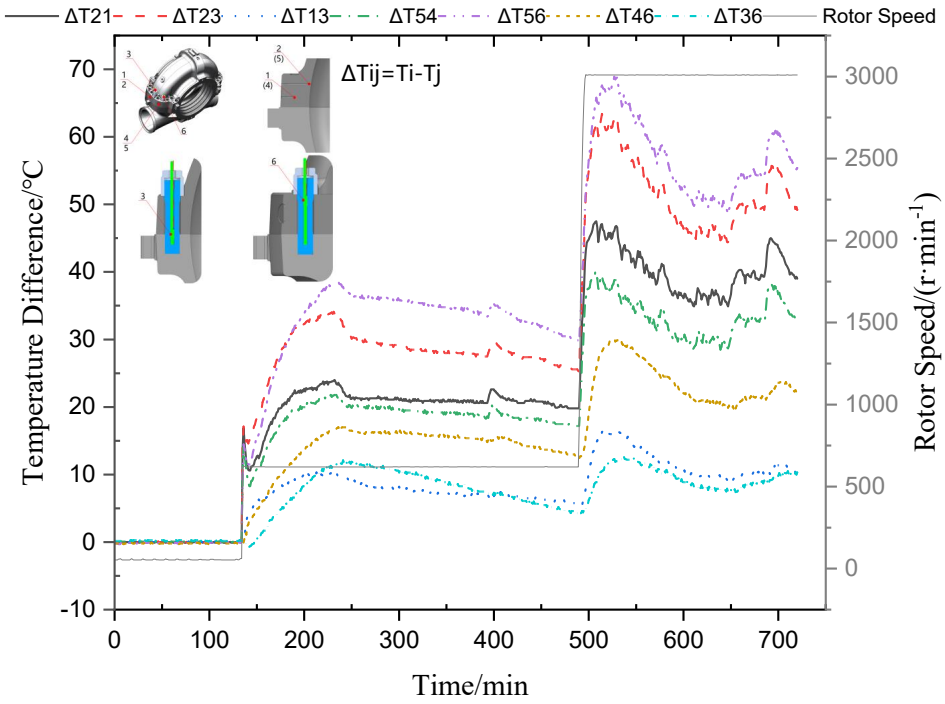

Figure 3 Diagram of the variation of temperature difference with time for the cold start method

The temperature difference curve between the measurement points in Figure 3 shows that ΔT21 represents the temperature difference or temperature gradient from the inner wall of the flange to the average thickness of the inner cylinder inlet area, while ΔT54 represents the temperature difference or temperature gradient from the inner wall of the flange to the average thickness of the inner cylinder discharge area. The maximum values of ΔT21 and ΔT54 during the rated speed idling phase are 48 °C and 40 °C respectively. ΔT23 indicates the temperature difference between the inner wall of the flange at the inlet area of the inner cylinder and 75% of the height of the bolt (near the mating surface of the flange in the upper and lower half of the cylinder); ΔT56 indicates the temperature difference between 99% of the depth (inner wall surface) of the flange near the discharge area of the inner cylinder and 25% of the height of the bolt (near the mating surface of the flange in the upper and lower half of the cylinder). The temperature difference between the flange 99% depth (inner wall surface) and the bolt 25% height (near the mating surface of the flange countersink nut) in the area of the inner cylinder discharge port.

Δ T13 characterises the temperature difference between 50% of the depth of the flange at the centre divider and 25% of the height of the bolt (near the mating surface of the flange countersink nut at the centre divider), with a maximum value of ΔT13 of 10 °C during the low speed warm-up phase and 15 °C during the rated speed idle phase. ΔT46 characterises the temperature difference between 50% of the depth of the flange near the discharge port of the inner cylinder and 25% of the height of the bolt (near the mating surface of the flange countersink nut at the centre divider). The temperature difference between 50% of the flange depth near the inner cylinder discharge port and 25% of the height of the bolt (near the centre

parting surface and the mating surface of the flange countersink nut) is measured at a maximum of ΔT46 of 15 °C during the low speed warm-up phase and 30 °C during the rated speed idle phase throughout the start-up period.

Combined with the measured data from the same depth and different positions of the flange in the inner cylinder, the temperature gradient along the axial direction of the unit is very small, i.e. T1 ≈ T4, T2 ≈ T5, so ΔT36 approximately characterises the temperature difference between a particular bolt at 75% height and 25% height position. Combined with Figure 3, it can be seen that the temperature difference between the different height positions of the bolts exhibits a non-linear fluctuating variation characteristic. During the entire start-up period, the maximum temperature difference between the low-speed warm-up phase and the rated speed idling phase ΔT36 is essentially the same, reaching 12 °C. On the one hand, the 75% height of the bolt is closer to the inlet port of the lower half of the inner cylinder, which is influenced by the high temperature inlet steam, and its temperature is higher than that of the 25% bolt height measurement point; on the other hand, the 25% height measurement point of the bolt is closer to the mating surface of the sink hole of the upper half of the inner cylinder, which is more influenced by the cooling of the lower temperature exhaust steam at the periphery. The temperature at the bottom of the bolt is higher than the temperature at the top.

Figures 4 and 5 compare the temperature rise and temperature rise rate at each stage of cold start. The temperature rise rate at measurement point 1 is denoted as Td1, and so on. Figure 4 shows that during the duration of 354 min low-speed warm-up period, the temperature of each measurement point rises from about 50 °C to about 200 °C. The temperature rise of measurement points 2 and 5 during this period is the largest, reaching 165.6 °C and 169.6 °C respectively; the temperature rise rate of each measurement point is about 0.45 °C/min for the flange and bolt in the inner cylinder, while Td5 is the largest, at 0.479 °C/min. The temperature rise rate of the flange was higher than that of the bolt. The temperature rise rate of the flange at 99% depth of the thickness is higher than that of the flange at 50% depth of the thickness, with the temperature rise rate Td satisfying Td2>Td1>Td3. The trend of Td4, Td5 and Td6 which on the outlet side of the inner cylinder is similar to that of the inlet side: Td5>Td4>Td6. See Figure 4.

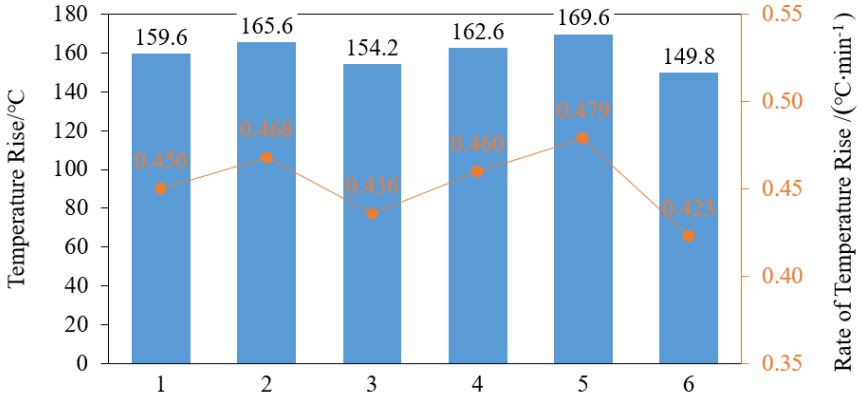

Figure 4 Temperature rise and temperature rise rate at each measurement point during the low-speed warm-up phase in cold start mode

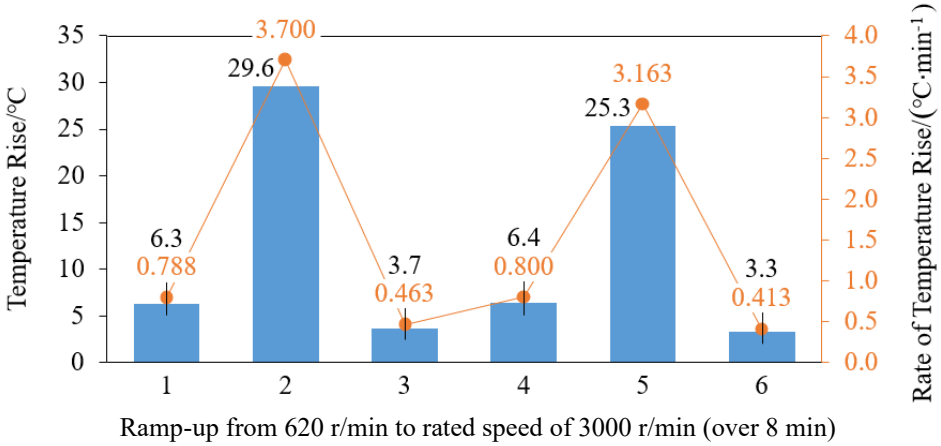

Figure 5 Temperature rise and rate of temperature rise at each measurement point during the ramp-up phase in cold start mode

Figure 5 summarises the temperature rise and temperature rise rate at each measurement point during the 8 min ramp-up from 620 r/min to the rated speed of 3000 r/min. The temperature rise at measurement points 2 and 5 during this period is the highest, reaching 29.6 °C and 25.3 °C respectively. Compared to Figure 4, the trend of temperature rise rate of each

measurement point during the ramp-up period is similar to that during the low-speed warm-up period: Td2>Td1>Td3, Td5>Td4>Td6. Compared to the low-speed warm-up period, the temperature rise rate of the corresponding measurement points during the ramp-up process has increased. The temperature rise rate at point 2 on the inner wall of the flange at the centre parting is 3.7 °C/min and at point 5 is 3.163 °C/min. Due to the very short stroke time, the temperature rise rate at 50% of the flange thickness and in the area of the bolt measurement points is an order of magnitude worse than the temperature rise rate at 99% of the flange thickness, and the response is slower, with the temperature rise rate on the inner wall of the flange being approximately eight times that of the bolt.

When the valve is opened, high temperature and high pressure superheated steam enters the inner cylinder through the valve, and the temperature of the metal of the flange and bolts in the inner cylinder is low under cold start. The heat is transferred from the inner wall surface to the interior. As the temperature of the inner wall surface rises and heat accumulates during start-up, the heat transfer between the inner wall surface and the steam changes from condensation to convection, and the heat transfer rate between the inner wall surface and the steam gradually decreases. At the moment of valve opening, the inner wall surface is the first to come into contact with the high temperature steam and the wall surface temperature rises rapidly, while the internal temperature is lower at this time.

Warm start-up

Figure 6 shows the temperature trend of each measurement point with the start-up time under warm start-up. At the early stage of warm start-up, the metal temperature of each measuring point of the flange-bolt of the inner cylinder is basically maintained at about 220 ℃. Here, the operating data of the unit from turning gear operation, warming up at low speed, ramping up to rated speed and carrying load to rated load, accumulating about 600 min, are selected for analysis. Similar to the cold start-up process, the warm start-up also requires a low-speed warm-up. The low-speed warm-up phase starts at 73 min and ends at 165 min, which takes about 92 min; then the rotor ramps up from 620 r/min to rated speed at 171 min (6 min for stroking); when it reaches 176 min, it starts to carry initial load and then gradually ramps up to rated load at 600 min. The low-speed warm-up time under warm start is 1/4 of the corresponding low-speed warm-up time under cold start, and the time required to ramp up from low-speed warm-up to the rated speed of 3000 r/min is basically the same, generally around 5 min.

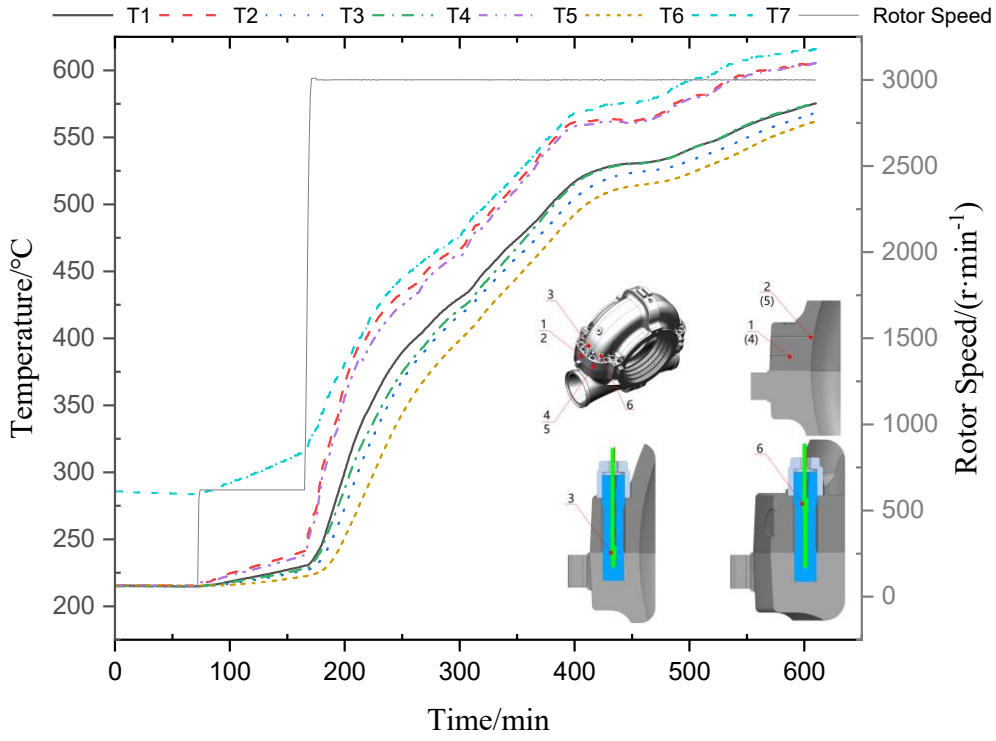

(a) Temperature variation of each measurement point over time during warm start-up

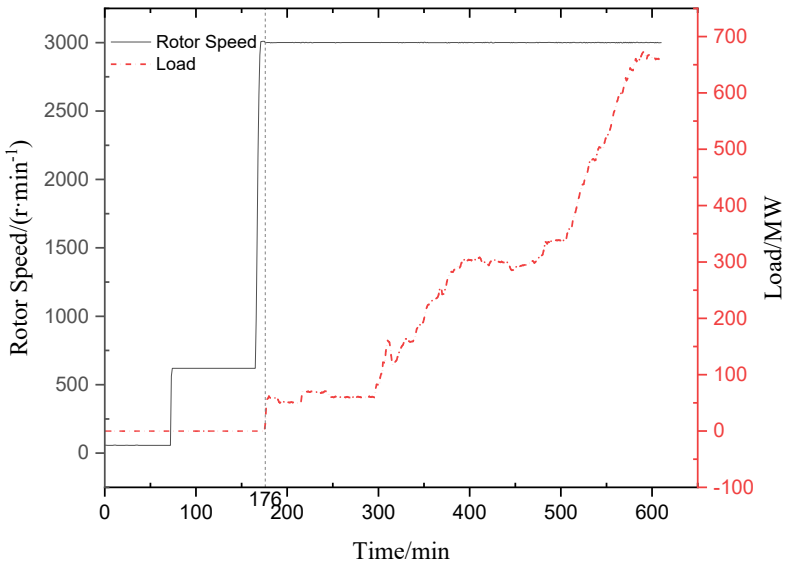

(b) Variation of unit load over time during warm start-up

Figure 6 Diagram of temperature and load variation with time under warm start

As can be seen from Figure 6, the metal temperature at each measurement point of the inner cylinder flange-bolt varies with the metal temperature at 99% of the depth of the main valve housing (characterising the inlet steam temperature of the inner cylinder). During the entire warm start-up time, the temperature of each measurement point satisfies the relationship T2≥T5>T1≥T4>T3>T6. In particular, after the initial load of the unit, the temperature distribution of measurement points 1 and 4, and measurement points 2 and 5 are basically the same during the ramp-up to rated load after the start-up time has accumulated to 400 min, and the change trend is also the same.

Figure 7 shows the trend of the temperature difference between the flange-bolt measurement points in the warm start-up mode. The maximum temperature difference is at the stage when the unit is ready to ramp up after the initial load, which corresponds to a cumulative start-up time of about 210 min, and the maximum value of ΔT56 is 110 °C.

In addition, the maximum temperature difference between the measurement points during the low-speed warm-up phase is within 15 °C, which is relatively small compared to the cold start. The temperature difference between the measurement points increases and then decreases and fluctuates randomly during the ramp-up to the rated speed and during the ramp-down to the rated load.

Δ T36, which characterises the temperature difference between the different heights of the bolts, follows the same pattern as for cold start, rising and then falling, then rising again and finally falling and levelling off at a certain value, showing a non-linear variation. The maximum temperature difference at the bolt measurement points during the low-speed warm-up phase is within 5 °C, while the maximum temperature difference during the ramp-up and load phase is approximately 28 °C.

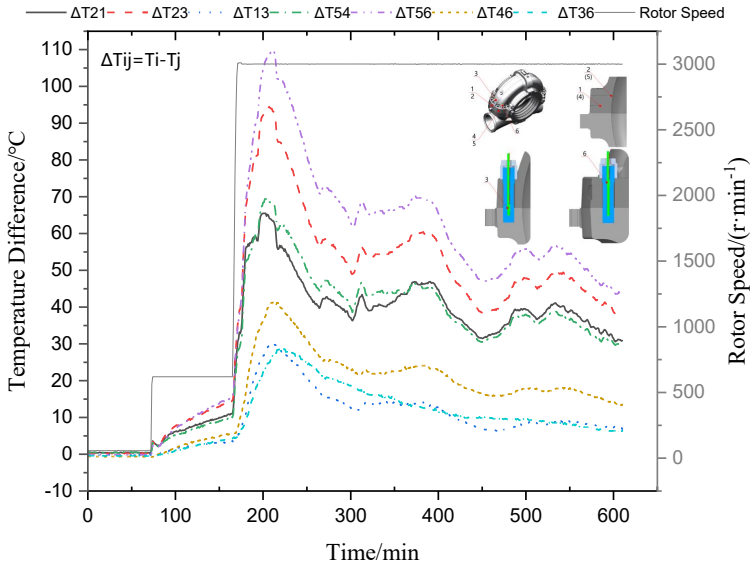

Figure 7 Schematic diagram of the temperature difference with time for the warm start method

Figures 8 and 9 compare the temperature rise and temperature rise rate of each measurement point during low-speed warm-up and ramp-up to rated speed phase under the warm start model, respectively. Compared to the cold start, the temperature rise at each measurement point is relatively small at each of these stages due to the higher initial temperature of the faceted flange-bolt in the warm start. The temperature rise and temperature rise rate of measurement points 2 and 5 are the largest, with values of 24.5 °C and 21.9 °C for the low-speed warm-up phase and 22.7 °C and 20.5 °C for the ramp-up phase, respectively; the corresponding temperature rise rates for each phase are 0.266 °C/min, 0.238 °C/min, 3.783 °C/min and 3.417 °C/min, respectively. The temperature rise rate of each measurement point satisfies Td2>Td1>Td3, Td5>Td4>Td6.

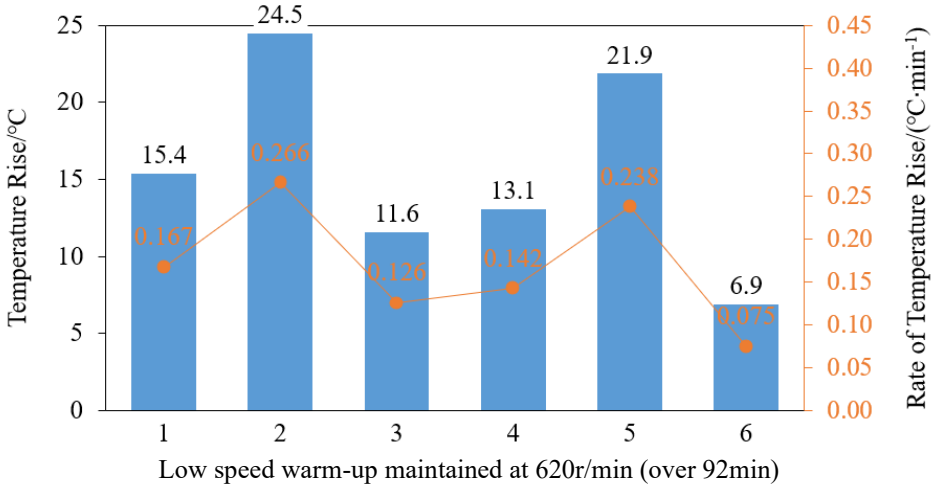

Figure 8 Temperature rise and rate of temperature rise at each measurement point during the low speed warm-up phase under the warm start mode

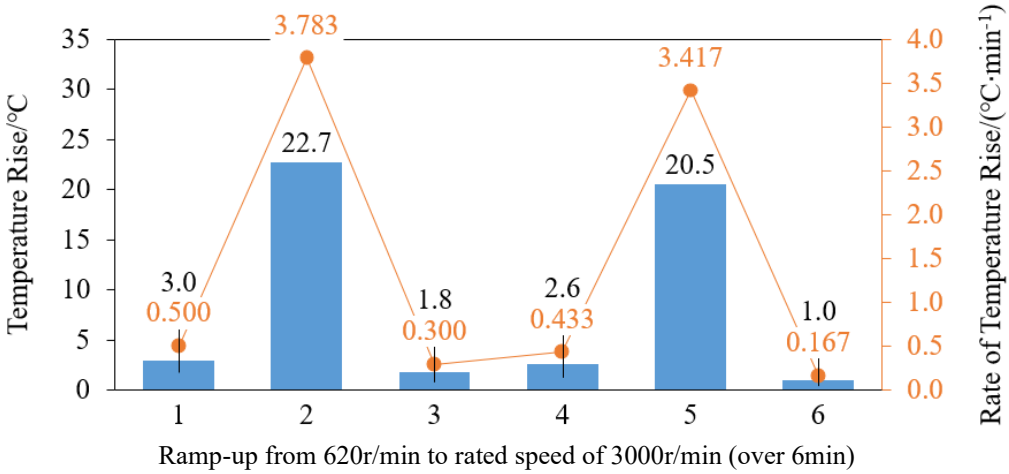

Figure 9 Temperature rise and rate of temperature rise at each measurement point during the ramp-up to rated speed phase under the warm start mode

Hot start-up

Figure 10 shows the temperature variation of each measurement point over time during a hot start. Unlike the cold and warm start methods, the temperature at each measurement point of the flange-bolt of the inner cylinder is basically maintained at about 390 °C during the hot start, so there is no need for low-speed warm-up. The unit's operating data from turning gear operation, ramp-up to rated speed and with initial load to rated load, accumulated for approximately 660 min, was selected for analysis. In the hot start mode, when the cumulative start time reaches 42 min, the unit starts to punch the rotor and reaches the rated speed of 3000 r/min at 51 min, and then starts to carry the load, and after about 5 min, the load reaches 10% of the initial load. During the cumulative start-up time of 400-660 min, the unit basically maintains more than 90% of the load and is close to the steady-state operation, during which the working temperature of the bolts is between 545 and 560°C.

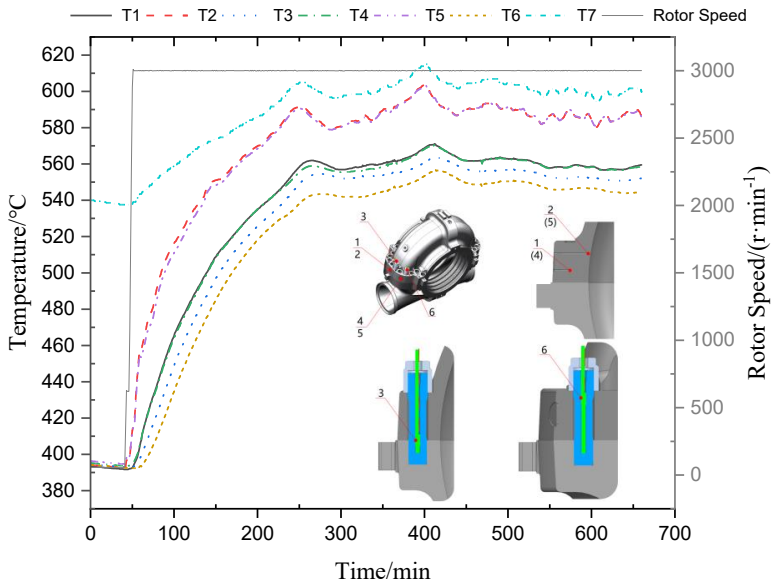

(a) Temperature variation of each measurement point over time during hot start-up

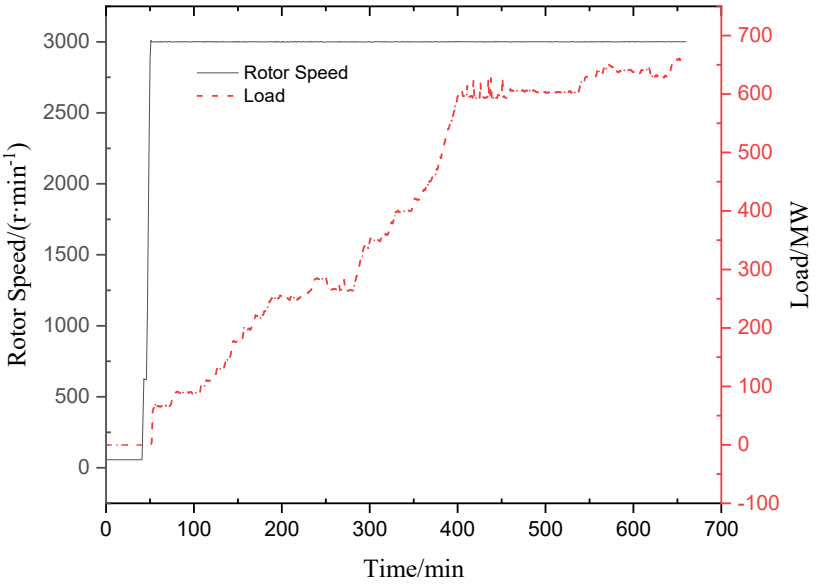

(b) Variation of unit load with time during hot start

Figure 10 Schematic diagram of temperature and load variation with time in the hot start mode

Combined with Figure 10, further analysis shows that, due to the similar installation position of measurement points 1 and 4, 2 and 5 in the flange area of the central division, their corresponding temperature distribution and change trends throughout the thermal start-up mode are the same, and the curves basically coincide, especially after the cumulative start-up time reaches 400 min, this characteristic is particularly obvious.

In addition, the fluctuating changes in the main steam parameters entering the inner cylinder mainly affect the temperature of the inner wall surface, such as T2, T5 changes in trend. By the flange and bolt heat transfer effect, measurement point temperature T1, T3, T4, T6 of this fluctuation change gradually weakened, especially into the steady state operation stage, the above measurement point temperature fluctuation change characteristics are basically eliminated, maintain in a certain value operation.

Figure 11 shows the trend of the temperature difference between the measurement points over time for the hot start method. The temperature difference between the measurement points under hot start is generally similar to that of cold start and warm start: the temperature difference curve first increases and then decreases, with the temperature of the measurement points on the inner wall surface fluctuating with the steam parameters entering the inner cylinder as it is closer to the steam side; the temperature fluctuations of the measurement points on the flange 50% depth and bolt side are not obvious and gradually stabilise. The maximum temperature difference occurs at 90 min, lagging behind the time when the unit starts to ramp up to 10% initial load (t=56 min), with a delay of about 34 min.

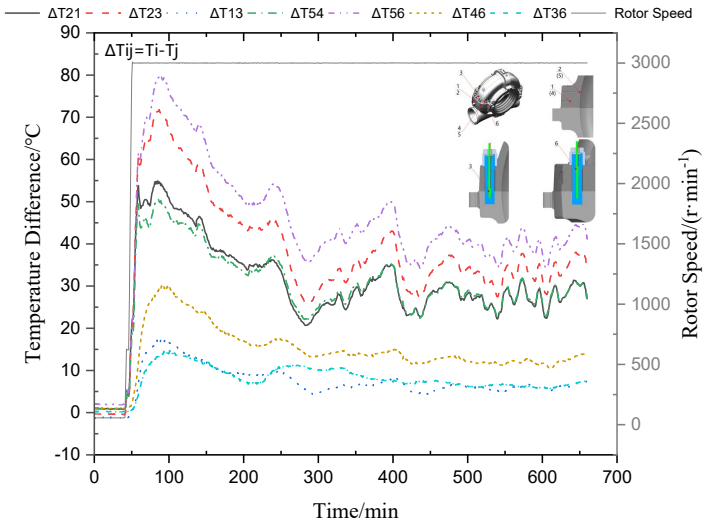

Figure 11 Diagram of the variation of temperature difference with time for the hot start method

The ΔT36, which characterises the temperature difference between the bolts at different heights, shows a non-linear pattern of increasing, then decreasing and finally converging to a certain value during the hot start mode. The maximum temperature difference at the bolt measurement point is 15 °C during the entire start-up cycle, which corresponds to the time when the unit is carrying 10% of the initial load; during steady-state operation, the bolt temperature difference remains at around 5 °C.

Figure 12 and Figure 13 compare the temperature rise and temperature rise rate of each measurement point during the ramp-up from coil to rated speed and from the start of load to the 10% initial load stage under hot start respectively. Similar to the cold start and warm start, the temperature rise and temperature rise rate of measurement points 2 and 5, which are closer to the steam side, are much higher than the other measurement points and satisfy Td2>Td1>Td3 and Td5>Td4>Td6. The temperature rise and temperature rise rate of the 99% depth measurement point of the flange is 2 orders of magnitude different from the bolt measurement point, and the bolt temperature changes more gently in the hot start mode and basically does not change during the speed rise phase. The temperature rise and temperature rise rate of measurement points 2 and 5 were the largest in the two phases, with temperature rise values of 22.8 °C, 19.8 °C; 26.9 °C, 25.8 °C; and temperature rise rates of 2.533 °C/min, 2.2 °C/min; 5.38 °C/min, 5.16 °C/min, respectively.

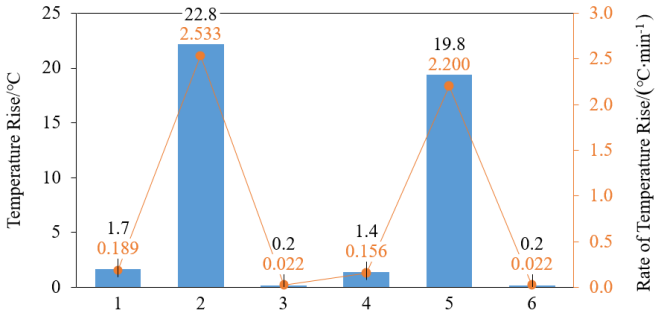

Ramp-up to rated speed of 3000 r/min from coil run (9 min)

Figure 12 Temperature rise and rate of temperature rise at each measurement point during the ramp-up from coil speed to rated speed in hot start mode

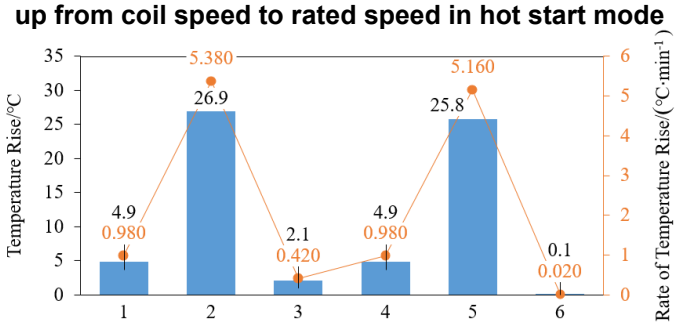

From start with load to 10% initial load (over 5 min)

Figure 13 Temperature rise and rate of temperature rise at each measurement point from start of load to 10% initial load in the hot start mode

Maximum temperature difference

In order to monitor the excessive transient thermal stresses in the flange-bolt structure of the cylinder during transients such as start-up due to temperature differences between components and deviations in the coefficient of thermal expansion of the material, the maximum temperature differences between the flange, flange-bolt and bolt heights were compared and analysed for different start-up methods. The maximum temperature difference ΔT between the measurement points during the entire start-up cycle for each typical start-up method is shown in Table 1.

Table 1 Summary of maximum temperature difference data between measurement points for each start-up method

Temperature difference	Maximum temperature difference/℃		
	Cold start-up	Warm start-up	Hot start-up
$\Delta T56$	70	110	80
$\Delta T23$	60	95	70
$\Delta T21$	48	65	55
$\Delta T54$	40	70	50
$\Delta T46$	30	40	30
$\Delta T13$	15	30	18
$\Delta T36$	12	28	15

The maximum temperature difference between the measurement points and the starting mode is shown in Figure 14. As can be seen from Figure 14, under the warm start-up model, the maximum temperature difference between the flange, the maximum temperature difference between the flange and the bolt and the maximum temperature difference between the different heights of the bolt are all higher than the corresponding temperature difference values of the cold start and the hot start. The maximum temperature difference between the bolts at different heights is ΔT36 at 28 °C.

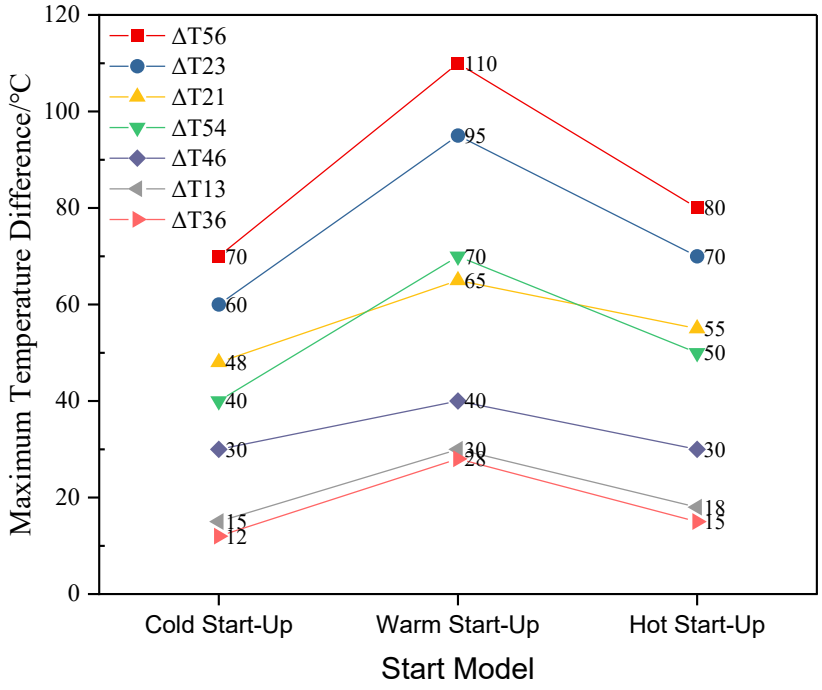

Figure 14 Curve of maximum temperature difference between measurement points versus start-up method

CONCLUSIONS

In this paper, the temperature and temperature difference variation law of the flange-bolt components of the joint surface under different starting methods is studied in conjunction with the field operation data of a steam turbine, and the following conclusions are drawn:

(1) When the operating state of the unit is changed, such as when the unit is ramped up to low-speed warm-up, ramped up to rated speed, ramped up to initial load and ramped up to rated load, etc., a large amount of high-temperature and high-pressure steam enters the inner cylinder because of the increase in the opening of the control vavle, which will cause a rapid change in the temperature of each measuring point of the flange-bolt on the middle division surface.

(2) Under the three typical start-up methods, the temperature difference between the flange-bolt measurement points shows a non-linear fluctuation with time, first increasing and then decreasing; during the whole start-up process, the moment of maximum temperature difference lags behind the moment when the operating condition of the unit changes; the corresponding lag time differs according to the start-up method and the location of the measurement points.

(3) For the 3 typical start-up methods, the temperature rise and temperature rise rate of the measured points is greatest at 99% depth of the flange, the temperature rise and temperature rise rate of the measured points at 50% depth of the flange is in the middle and the temperature rise and temperature rise rate of the measured points of the bolt is the least.

(4) In the warm start mode, the maximum temperature difference between the flanges of the central parting face, the maximum temperature difference between the flanges and the bolts and the maximum temperature difference between the different heights of the bolts are all higher than the temperature difference values corresponding to the cold start and the hot start modes; the maximum temperature difference between the flanges and the bolts is ΔT56 with a maximum temperature difference value of 110°C; the maximum temperature difference between the flanges is ΔT54 with a maximum temperature difference value of 70°C; the maximum temperature difference between the different heights of the bolts is ΔT36 with a maximum temperature difference value of 28°C;

(5) Under the hot start mode, the temperature difference between 75% of the height of the bolt and 25% of the height of the bolt is basically maintained at about 5 ℃ during stable operation at 90% of the load, and the temperature gradient of the bolt along the axis direction is relatively small, so the steady state service temperature of the bolt can be characterized by the measured temperature at 75% of the height of the bolt, and its design and selection; the steady state service temperature of the bolt at this stage is distributed between 545 ~ 560 ℃.

REFERENCES

Zhao Bin, Wang Zhe, Yan Chen shuai, Dong Chang wei, Bao Siyu, Lyu Xiao biao and Zhou Xing yu (2022), Thermal economy analysis on deep peak regulation operation of supercritical 600MW coal-fired unit. *Thermal Power Generation,* 51(1):109-114.

Yu Jian liang, Yan xing qing and Luo cong ren (2013), Temperature distribution and bolt load changes of flange system in high temperature. *Pressure Vessel Technology*, 30(11):1-7.

Yu Jiu yang, Wang Ming wu, Zheng Xiao tao and Cheng Shi (2014), Temperature field analysis of flanged joints at high temperature based on finite element method. *Journal of Wuhan Institute of Technology*, 36(10):31-36.

Hao Zhen zhen and He Chuang xin (2016), Conjugate heat transfer of high temperature bolts on integral inner casing of steam turbines in H-class CCPP. *Thermal Turbine*, 45(4):265-268.

Jiang Feng, Yang Xi, Zhao Wei le, Zhou Wen hai, Chen Fei and Yu Rui li (2021), Study on sealing performance of flange in valve under transient temperature fluctuation. *Fluid Machinery*,49(3):34-39.

Wu Shi fang, kang Ming, Zhang Jun hui and Li Xiao xiao (2021), Temperanture field measuremen and analysis of IP inner casing inlet chamber. *Journal of Chinese Society of Power Engineering*, 41(6):446-451.

Nailong Zhao, Weizhe Wang, Hui Hong, Richard Amankwa Adjei and Yingzheng Liu (2016), Mechnical behavior study of steam turbine casing bolts under in-service conditions. *Proceedings of ASME turbo Expo 2016*, GT2016-56723.

Benjamin Leibing, Andreas Klenk and Michael Seidenfuss (2019), Component testing and numericl calculation of a bolted high temperature power plant pipe flange under complex, near-service loads, *Journal of pressure vessel technology,* 141:061201-11.

Wolfgang F. Mohr and Paolo Ruffino (2012), Experimental investigation into thermal behavior of steam turbine components: Part 1—temperature measurements with optical probes. *Proceedings of ASME turbo Expo 2012*, GT2012-68703.

Gabriel Marinescu and Andreas Ehrsam (2012), Experimental investigation into thermal behavior of Steam Turbine components: Part 2—natural cooling of steam turbines and the impact on LCF life. *Proceedings of ASME turbo Expo 2012*, GT2012-68759.

Gabriel Marinescu, Michael Sell, Andreas Ehrsam and Philipp B. Brunner (2013), Experimental investigation into thermal behavior of steam turbine components: Part 3 — Startup and the Impact on LCF Life. *Proceedings of ASME turbo Expo 2013*, GT2013-94356.

Gabriel Marinescu, Peter Stein and Michael Sell (2014), Experimental investigation into thermal behavior of steam turbine components: Part 4 — Natural Cooling and Robustness of the Over-Conductivity Function. *Proceedings of ASME turbo Expo 2014*, GT2014-25247.